Available online at www.sciencedirect.com
SCIENCE DIRECT®
Catalysis Today 93–95 (2004) 675–680
CATALYSIS TODAY
www.elsevier.com/locate/cattod

Comparative study on the acidic and catalytic properties of AlMSU-2- and AlMCM-41-like samples: both synthesized from the same zeolite-like precursor

Shangru Zhai [a], Junlin Zheng [a], Xi'e Shi [a,b], Ye Zhang [a], Liyi Dai [b], Yongkui Shan [b], Mingyuan He [b], Dong Wu [a], Yuhan Sun [a,*]

[a] *State Key Laboratory of Coal Conversion, Institute of Coal Chemistry, Chinese Academy of Sciences, Taiyuan 030001, PR China*
[b] *Department of Chemistry, East China Normal University, Shanghai 200063, PR China*

Available online 8 August 2004

Abstract

The objective of this work is to give a comparative characterization of the three-dimensional (3D) MSU-2 and unidimensional (1D) MCM-41-like aluminosilicates, in particular with respect to acidity and catalytic properties in 1,3,5-triisopropylbenzene cracking. Mesoporous AlMSU-2 with wormhole but uniform pores and large surface area, previously obtainable only from silicon alkoxides, has been successfully prepared from pre-assembled zeolite-like units in the presence of nonionic octyl-phenyl polyethylene ether (TX-100) as template through a $N^0(N^+)X^-I^+$ pathway in strong acid media. For comparison purpose, hexagonally ordered AlMCM-41 was also synthesized from the same inorganic precursor with cetyltrimethylammonium bromide (CTAB) as template under mild basic conditions. Catalytic results in bulky 1,3,5-triisopropylbenzene cracking showed that the 3D AlMSU-2 was much more active than the hexagonally packed AlMCM-41 though both materials were synthesized from the same precursor and presented similar acid strength.

Keywords: Mesoporous; Synthesis; Characterization; Catalysis

1. Introduction

Mesoporous silicas with wormhole framework structures such as MSU-X family [1,2] are generally more active heterogeneous catalysts in comparison to their ordered hexagonal analogs (e.g. MCM-41 [3] and SBA-15 [4]). The enhanced activity has been attributed to, in part, a pore network that is connected in three dimensions, allowing the guest molecules to more readily access reactive sites that have been designated into the framework surface [5]. It is found that, however, previously reported studies on MSU-X materials were mainly devoted to the preparation of inactive purely siliceous [1,2,6–11], organically modified [12–18] or MSU-X thin membranes [19]. There are very few reports on the preparation of Al-containing MSU-X materials [20] though it is highly possible to obtain catalysts with remarkably different acid surface chemistry because of theirs unique 3D wormhole mesostructures. This may be attributed to the non-electrostatic assembly preparation conditions (usually performed under neutral, near-neutral pH and ambient reaction conditions) of MSU-X materials, under which it is very difficult to prepare MSU-X containing heteroatoms in the framework or even a little amount can be incorporated the condensation between the metal species and silica precursor is incomplete. In regard to acid catalysis, as we know, silica MSU-X is of limited use, owing to the absence of active sites. Therefore, it is greatly significant to introduce Al atoms into the framework of MSU-X. Although Bagshaw et al. [20] have prepared AlMSU-2 employing $Al_2(SO_4)_3{\cdot}18H_2O$ and costly tetraethylorthosilicate (TEOS) as the aluminum and silica source with TN-101 as template, acidic and catalytic properties of the obtained materials were not involved in the literature.

Recently, a large number of strategies have been reported to improve the activity of mesoporous aluminosilicates in acid-catalyzed reactions. One of such efficient approaches consists in mimicking the physicochemical conditions prevalent in the synthesis gels from which zeolite materials are

* Corresponding author. Tel.: +86 351 4063121; fax: +86 351 4041153.
E-mail address: yhsun@sxicc.ac.cn (Y. Sun).

0920-5861/$ – see front matter © 2004 Elsevier B.V. All rights reserved.
doi:10.1016/j.cattod.2004.06.034

obtained, and promoting the surfactant-assisted assembly of the zeolite precursors present in the gel. In this way, mesostructures analogous to MCM-41 and SBA-15 characterized by enhanced activity have been obtained from Y, MFI, BETA and L preformed zeolite precursors [21–28]. For instances, Pinnavaia and co-workers reported the synthesis of AlMSU-S assembled from a zeolite Y [21], BETA [22,25] and MFI seeds solution [22,25]; Xiao and co-workers depicted mesoporous aluminosilicates of MAS-3 [28], MAS-5 [23], MAS-7 [24], MAS-8 [28] and MAS-9 [26] structured by pre-assembled L, BETA, MFI precursors in the presence of CTAB or nonionic $EO_{20}PO_{70}EO_{20}$ (P127) as surfactants.

It is found that, however, these materials are all composed of 1D channels, from the catalysis and reaction kinetics point of view, inferior to aluminosilicates with 3D pore structures such as Al-incorporated MSU-X, and mesoporous AlMSU-X assembled from pre-formed zeolite precursors have not been found yet. We report here the preparation of mesoporous AlMSU-2 with 3D uniform wormholes from the pre-formed zeolite-like precursor in strongly acidic media. To better illustrate its advantageous pore structures in catalysis, well-ordered AlMCM-41-like sample was also synthesized from the same precursor. Both samples were thoroughly characterized by means of XRD, HRTEM, N_2 sorption, ^{27}Al-NMR, NH_3-TPD and pyridine-IR. Furthermore, catalytic cracking of 1,3,5-triisopropylbenzene has been investigated over both materials. Our results showed that the 3D AlMSU-2 was more active in the cracking reaction than its ordered counterpart though both materials with the similar Si/Al ratio and acid strength.

2. Experimental

2.1. Synthesis of AlMSU-2

The preparation of AlMSU-2 consists of two steps.

In the first step, a beta precursor solution with a molar composition of Al_2O_3:20.0 TEAOH:2.11 Na_2O:44.44 SiO_2:613 H_2O was prepared mainly adapted from the literature [23]. Typically, 2.40 g of fumed silica was dissolved in a mixture containing 10.58 g of a 25 wt.% TEAOH aqueous solution, 0.158 g of $NaAlO_2$, 0.08 g of NaOH and 2.00 g of distilled water. After further stirring for 4 h, the opalescent gel was poured into an autoclave and heated at 140 °C for 6 h.

In the second step, the synthesis of AlMSU-2 was carried out as follows: (1) 6.99 g of TX-100 was dissolved into 144 ml H_2O under stirring at room temperature. (2) The obtained pre-assembled beta seeds was poured into the above surfactant solution, followed by quick addition of determined amount of HCl (11.96 M) to give a gel with molar ratio of SiO_2:0.0225 Al_2O_3:0.45 TEAOH:0.047 Na_2O:0.27 TX-100:7.2 HCl:213.8 H_2O. (3) The gel was further stirred for 6 h and then the precipitate was filtered, washed thoroughly with water and re-dispersed in distilled water with 1.0 g/20 ml ratio and transferred into an autoclave for additional reaction at 110 °C for 48 h. The final product was collected by filtration, water washed, dried and calcined in air at 550 °C for 6 h. The acid form was obtained by ion-exchange with 1.0 M NH_4NO_3 at 80 °C for 12 h followed by activation at 550 °C for 4 h.

2.2. AlMCM-41 preparation

Typical synthesis of AlMCM-41-like material was carried out as follows: (1) 2.92 g of CTAB was dissolved in 79.2 ml H_2O under stirring. (2) The obtained pre-formed zeolite seeds was poured into the above surfactant solution, followed by adding determined content of H_2SO_4 (6 M) over about 1 h to adjust the pH to 9. (3) The white mixture was further stirred for 2 h and loaded into an autoclave for crystallization at 140 °C for 48 h. The rest of procedures were completely similar to that for AlMSU-2.

2.3. Characterization

XRD patterns were recorded at room temperature on a Rigaku D Max III VC instrument with Ni filtered Cu Kα radiation, in the 2θ range of 1.2–10° at a scan rate of 1°/min. TEM images were taken on a Jeol Model 1200 EX instrument operated at an accelerating voltage of 200 kV. The specific surface areas of the samples were determined by BET method using N_2 adsorption measured with a TriStar 3000 analyzer. Prior to the adsorption, the samples were activated at 150 °C for 6 h at 10^{-4} Torr. ^{27}Al-NMR experiments were performed on a Bruker MSL 300-WB spectrometer, in a 7 mm zirconia rotor at 4.0 kHz and 11.7 T. Chemical shifts were measured with respect to $Al(H_2O)_6^{3+}$ as the reference. Al contents in the samples were determined by Perkin-Elmer 3300 DV ICP and NMR technique. NH_3-TPD was performed on 200 mg of each catalyst with argon (40 ml/min) as the carrier gas and a TCD as the detector. NH_3-TPD curves was obtained in the range 120–600 °C with a linear heating rate of 10 °C/min. IR-pyridine adsorption was obtained on Impact 410, Nicolet spectrometer. The self-supporting wafers about 5 mg/cm^2 were evacuated in situ in an IR cell under vacuum (10^{-5} Torr) at 400 °C for 4 h and cooled to room temperature, then pyridine was exposed to the disks. After the adsorption at room temperature for 0.5 h and evacuation at 150 °C for 0.5 h, the spectra were recorded.

2.4. Catalytic test

1,3,5-Triisopropylbenzene cracking was carried out at 300 °C by pulse method to evaluate catalytic performance of both samples. In each run, 60 mg of catalyst was used, the pulse injection of the reactant was 0.2 μl, and nitrogen was used as carrier gas at a flowing rate of 50 ml/min. The reaction products were analyzed using GC-9A gas chromatograph (Shimadzu Co.) equipped with FID and a high-resolution Chrom-Workstation Data Set.

Table 1
Physicochemical properties of AlMSU-2- and AlMCM-41-like samples

Sample	Si/Al	d_{100} (nm)	S_{BET} (m^2/g)	Pore size (nm)	Pore volume (cm^3/g)	Wall thickness (nm)
AlMSU- 2	23	4.5	800	2.26	0.44	2.94
AlMCM-41	21	4.1	726	2.76	0.89	1.97

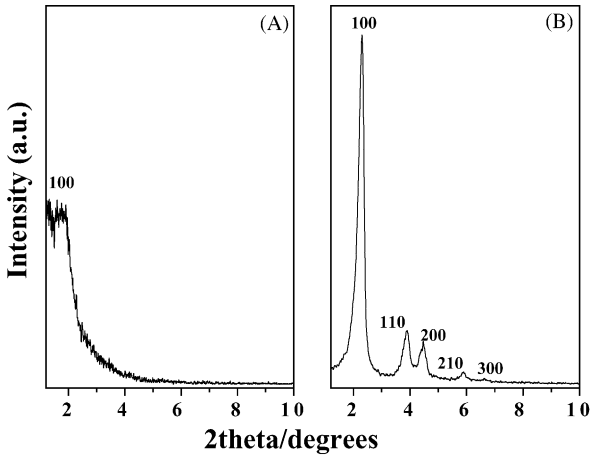

Fig. 1. XRD patterns of calcined (A) AlMSU-2- and (B) AlMCM-41-like samples.

3. Results and discussion

3.1. XRD and HRTEM

Table 1 gives textural properties of the resultant mesoporous aluminosilicates. Despite incorporating large amount of Al, the textural properties of AlMSU-2 are similar to those of MSU-X [1]. Fig. 1 shows XRD patterns of calcined AlMSU-2- and AlMCM-41-type aluminosilicates. Clearly, the pattern for AlMSU-2 exhibits only a single broad peak reflection, which is typical of disordered pore structures with no long-range symmetry, and similar to those MSU-X silicas assembled from the same surfactant but only with TEOS or sodium silicates as the starting source [1,29]. In contrast, the pattern of AlMCM-4 shows an intense (1 0 0) peak and several higher order (1 1 0), (2 0 0), (2 1 0) and (3 0 0) lines, characteristic of a hexagonally ordered specimen [30].

TEM images in Fig. 2 show randomly packed of 3D mesoporous channels and ordered arrangement of 1D cylindrical channels for AlMSU-2- and AlMCM-4-type samples, and confirm that both samples have 3D wormhole and 1D hexagonal structures as do MSU-X [1] and MCM-41 [3], respectively.

3.2. N_2 sorption studies

Nitrogen sorption isotherms and corresponding pore size distributions of both samples are displayed in Fig. 3. Obviously, both isotherms are type IV curves according to the IUPAC classification, and are typical for well-defined mesoporous frameworks [3]. For AlMCM-41-like sample, it possesses a distinct jump of capillary condensation in the mesopores at $P/P_0 = 0.25$–0.45 and a steep increase adsorption zone at high relative pressure of 0.8–1.0 due to the textural porosity. The inflection point of this isotherm is situated at $P/P_0 \sim 0.35$, and the different stages are clearly separated. In contrast, the isotherm for AlMSU-2 not only indicates a much lower adsorption capacity, but also a less well-defined inflection point shifted to lower relative pressures (~0.15), which can be assigned to its smaller pore size and pore volume in comparison with the AlMCM-41-like sample (see Table 1).

Correspondingly, pore size distributions inserted in Fig. 3 show two uniform pores of 2.26 and 2.76 for the both calcined samples, respectively. Combined with XRD results, we roughly estimate the pore wall thickness of both materi-

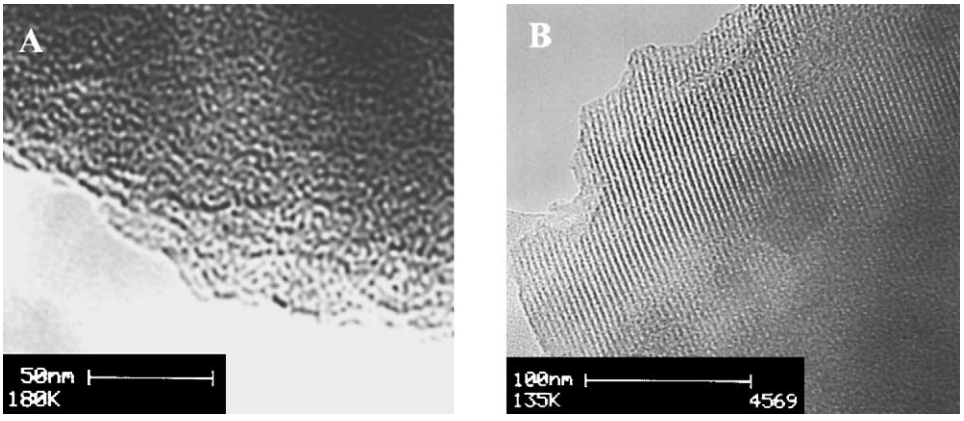

Fig. 2. TEM images of (A) disordered AlMSU-2 and (B) highly ordered AlMCM-41-like samples.

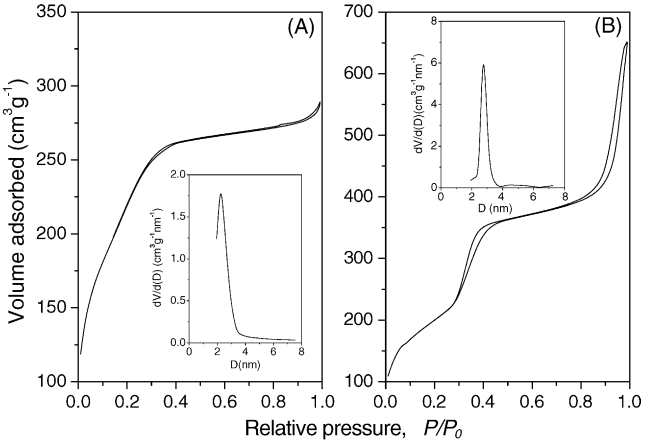

Fig. 3. N_2 sorption isotherms and corresponding pore size distributions (inset) of (A) wormhole AlMSU-2 and (B) hexagonal AlMCM-41-like materials.

als is 2.94 and 1.97 nm [31], respectively. The results are in good agreement with those of reported studies that the wall thickness of mesoporous materials templated by neutral surfactants is larger than that of mesostructures such as M41S family obtained from ionic surfactants [1,4].

3.3. ^{27}Al-NMR

It has been well demonstrated that ^{27}Al chemical shifts vary with not only the coordination number of the aluminum species but also the type of ligands [32–35]. Shown in Fig. 4 are the ^{27}Al-NMR spectra of AlMSU-2- and AlMCM-41-type samples. Distinctly, AlMSU-2 has a strong line at 58 ppm with a shoulder peak at 0 ppm, assigned to 4- and 6-coordinated Al atoms, respectively. Similarly, AlMCM-41-like material also exhibits a main peak at 57.5 ppm and a very small peak at 0 ppm, attributed to 4- and 6-coordinated Al species, respectively. The almost completely similar chemical shifts of both 4- and 6-coordinated Al species observed in both materials are probably due to the sameness of coordinate ligands, which may be attributed to they are structured by the same inorganic precursor. In addition, there are more 6-coordinated Al atoms in AlMSU-2 than its hexagonal counterpart. This observation may be resulted from the different preparation routes, i.e., AlMSU-2- and AlMCM-41-like samples were obtained under strong acid and maid basic conditions, respectively. As well known, under strong acidic conditions, it is a challenge to incorporate Al into the framework of mesostructures due to the existence of H^+ which can easily make Al dealuminate from framework or even dissolve into the reaction solution [4,24]. However, it is clearly seen from this work that Al species have been easily introduced into AlMSU-2 in strong acid media with pre-formed nanosized Al–O–Si units as the inorganic source.

Additionally, it is interesting that chemical shift of 4-coordinated Al in the AlMSU-2 is 58 ppm rather than 51 ppm reported for AlMSU-2 obtained by conventional methods [20], indicating that Si–O–Al environments in our AlMSU-2 are different from those commonly present in the amorphous AlMSU-2 [20].

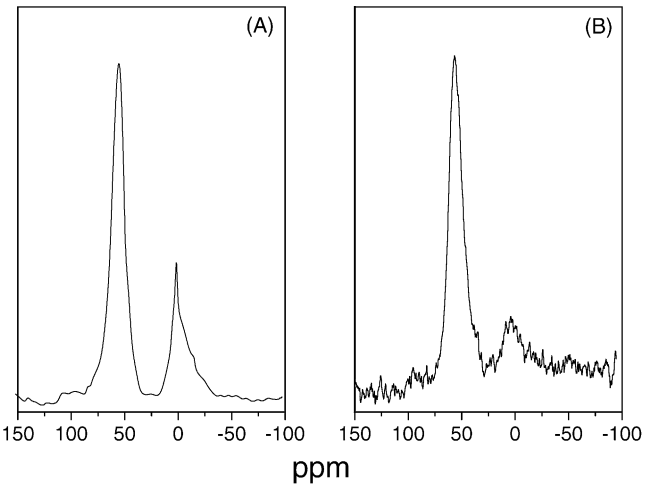

Fig. 4. ^{27}Al-NMR spectra of (A) AlMSU-2- and (B) AlMCM-41-type samples.

3.4. NH_3-TPD and pyridine-IR

Fig. 5 illustrates NH_3-TPD profiles of both samples in the acid form, while the temperature desorption maxima are also given. Interestingly, the desorption curves of both samples consist of three distinct peaks at around 204, 299 and 391 °C, respectively. Whereas the lower temperature

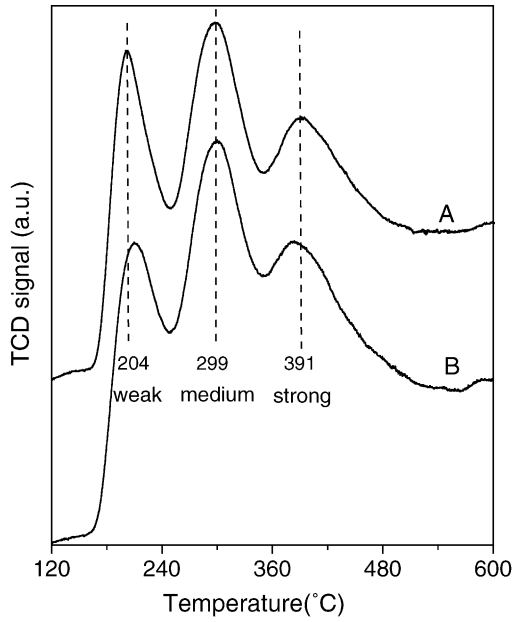

Fig. 5. NH_3-TPD profiles of the ion-exchanged (A) AlMSU-2- and (B) AlMCM-41-like products.

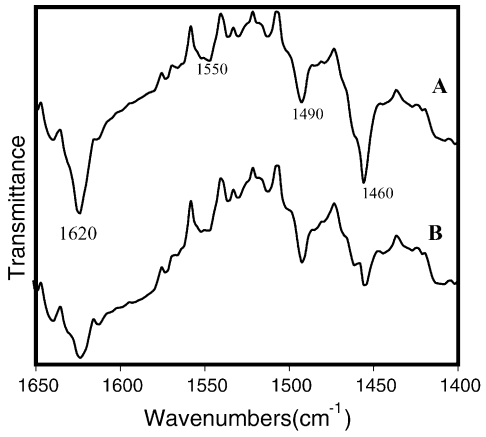

Fig. 6. IR spectra of pyridine adsorbed on (A) wormhole AlMSU-2 and (B) well-ordered AlMCM-41-like samples after they have been degassed under vacuum at 150 °C for 0.5 h.

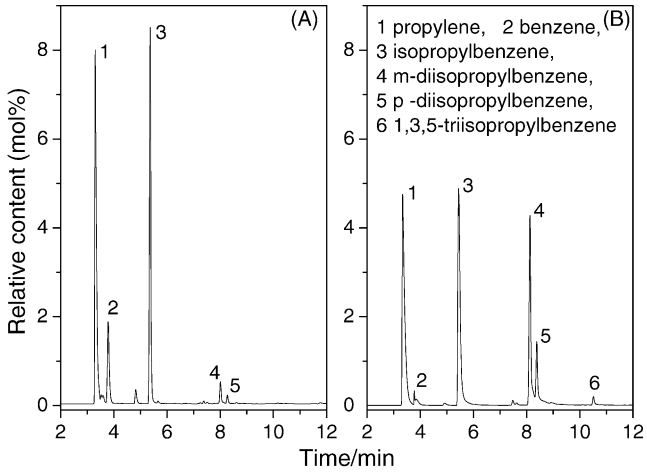

Fig. 7. Product distribution and relative content (mol%) in 1,3,5-triisopropylbnezene cracking over (A) wormhole AlMSU-2 and (B) hexagonal AlMCM-type catalysts at 300 °C.

peak (204 °C) can be attributed to physisorbed and weakly bonded ammonia molecules [36,37], the second and third peaks are ascribed to ammonia molecules desorbed from medium and strong acid sites [38,39], respectively. The total acid amounts on both materials are almost identical, which is measured by the ratio of total three TPD peaks areas of AlMSU-2 to that of AlMCM-41, and the ratio value is about 1.10. It is also stated that, regardless of their acid sites numbers, both samples present similar acid strength, which is reasonably assigned to them obtained from the same pre-assembled units [40].

IR spectra of pyridine adsorbed on ion-exchanged AlMSU-2- and AlMCM-41-like samples are shown in Fig. 6. It can be clearly seen that both catalysts exhibit similar bands at 1460, 1490, 1550 and 1620 cm^{-1}. According to the recent studies [35,41], the bands at 1460 and 1620 cm^{-1} are attributed to Lewis acid sites, the band at 1560 cm^{-1} is assigned to Brönsted acid centers, and the band at 1490 cm^{-1} is ascribed to a combinational signal associated with both Lewis and Brönsted acid sites.

It is interesting to note that at the same temperature AlMSU-2 exhibits much higher concentration of Lewis acid sites than those of AlMCM-41-type sample, although their Brönsted acid centers are almost identical. These results are well consistent with the aforementioned ^{27}Al-NMR observations, i.e., more Al species are non-framework in AlMSU-2 than those of AlMCM-41-like sample due to its strong acid preparation route, which is well consistent with those results reported before [24].

3.5. Catalytic test

Product distributions and relative content in 1,3,5-triisopropylbenzene cracking over both AlMSU-2- and AlMCM-41-like samples are illustrated in Fig. 7. Obviously, both catalysts show very high activities in 1,3,5-triisopropylbenzene cracking and give high conversion of 100 and 99.08%, respectively. Conclusively, using 1,3,5-triisopropylbenzene as the model feed, with a kinetic diameter of 0.94 nm and therefore there is no geometrical hindrance to the inner active sites of both samples due to their large mesopores of 2.26 and 2.76 nm, respectively.

It is interesting to note that although both materials show high activities in 1,3,5-triisopropylbenzene conversion, product distributions over them are substantially different. Over AlMSU-2, propylene, benzene and isopropylbenzene are major products and selectivity for them is 44.15, 11.89 and 40.36%, respectively, whereas there are very small amounts of *m*- and *p*- diisopropylbenzene isomers. It is therefore considered that 1,3,5-triisopropylbenzene is almost completely cracked to isopropylbenzene, and furthermore, large part of isopropylbenzene was decomposed into propene and benzene (see Fig. 7A). In contrast, over the AlMCM-41-like sample, propylene, isopropylbenzene and *m*-diisopropylbenzene are main products and selectivity for them is 35.36, 33.97 and 22.34%, respectively, revealing 1,3,5-triisopropylbenzene is principally cracked to isopropylbenzene and diisopropylbenzene (see Fig. 7B). It is thus deduced that 1,3,5-triisopropylbenzene is cracked by far more completely over the 3D worm-like AlMSU-2 than over the 1D ordered AlMCM-41-like material. Possibly, the unique 3D wormhole pore structures of AlMSU-2 play the key role leading to deeper cracking of 1,3,5-triisopropylbenzene [42].

As investigated by Xiao and co-workers [43], under optimal conditions, AlMCM-41-like MAS-5 exhibits a very high cracking activity for bulky hydrocarbon such as 1,3,5-triisopropylbenzene. Here our work shows that this AlMSU-2 has an even much higher catalytic activity than AlMCM-41-like material MAS-5, suggesting that AlMSU-2 may be a helpful catalyst for catalytic cracking of bulky residue.

4. Conclusions

In summary, an active mesoporous aluminosilicate with wormhole but uniform pore structures (AlMSU-2) has been firstly synthesized via the co-templates of TEAOH and neutral TX-100 under strongly acidic conditions. For comparison purpose, a structurally ordered hexagonal AlMCM-41-like sample has also been prepared using the same pre-assembled zeolite-like units as for AlMSU-2 mainly followed the reported method [23]. Catalytic results in 1,3,5-triisopropylbenzene cracking showed that although both catalysts presented similar acid strength and led to high conversion of 1,3,5-triisopropylbenzene, the cracking extent of the reactant over AlMSU-2 was by far deeper than that over AlMCM-41-type material, whereas both samples with similar Si/Al ratio. It was possible that the wormhole framework structures of AlMSU-2 played the important role leading to deeper cracking less diisopropylbenzene in the product, suggesting it may find a wide application in catalytic cracking of bulky hydrocarbons.

Acknowledgements

Financial support from the National Key Basic Research Special Foundation of China (No. 2000048001) and Natural Science Foundation of China (29973057) is gratefully acknowledged.

References

[1] S.A. Bagshaw, E. Prouzel, T.J. Pinnavaia, Science 269 (1995) 1242.
[2] S.A. Bagshaw, T.J. Pinnavaia, Angew. Chem. Int. Ed. 35 (1996) 1102.
[3] C.T. Kresge, M.E. Leonowica, W.J. Roth, J.C. Vartuli, J.S. Beck, Nature 359 (1992) 710.
[4] D. Zhao, J. Feng, Q. Huo, N. Melosh, G.H. Fredrickson, B.F. Chmelka, G.D. Stucky, Science 279 (1998) 548.
[5] E. Prouzet, F. Cot, G. Nabias, A. Larbot, P. Kooyman, T.J. Pinnavaia, Chem. Mater. 11 (1999) 1498.
[6] S.S. Kim, T.R. Pauly, T.J. Pinnavaia, Chem. Commun. (2000) 835.
[7] G. Herrier, J.L. Blin, B.L. Su, Langmuir 17 (2001) 4422.
[8] C. Boissiere, A. Larbot, E. Prouzet, Chem. Mater. 12 (2000) 1937.
[9] M.D. Mcinall, J. Scott, L. Mercier, P.J. Kooyman, Chem. Commun. (2001) 2282.
[10] C. Boissiere, M.A.U. Martines, M. Tokumoto, A. Larbot, E. Prouzet, Chem. Mater. 15 (2003) 509.
[11] J.W. Lee, J.Y. Kim, T.H. Hyeon, Chem. Commun. (2003) 1138.
[12] R. Richer, L. Mercier, Chem. Commun. (1998) 1775.
[13] J. Brown, R. Richer, L. Mercier, Micropor. Mesopor. Mater. 37 (2000) 41.
[14] Y.J. Gong, Y. Li, D. Wu, Y.H. Sun, Catal. Lett. 74 (2001) 213.
[15] Y.J. Gong, Z.H. Li, D. Wu, Y.H. Sun, F. Deng, Q. Luo, Y. Yue, Micropor. Mesopor. Mater. 49 (2001) 95.
[16] R. Richer, L. Mercier, Chem. Mater. 13 (2001) 2999.
[17] A. Bibby, L. Mercier, Chem. Mater. 14 (2002) 1591.
[18] L. Beaudet, K.Z. Hossain, L. Mercier, Chem. Mater. 15 (2003) 327.
[19] C. Boissiere, M.A.U. Martines, P.J. Kooyman, T.R. de Kruijff, A. Larbot, E. Prouzet, Chem. Mater. 15 (2003) 460.
[20] S.A. Bagshaw, T. Kemmitt, N.B. Milestone, Micropor. Mesopor. Mater. 22 (1998) 419.
[21] Y. Liu, W. Zhang, T.J. Pinnavaia, J. Am. Chem. Soc. 122 (2000) 8791.
[22] Y. Liu, W. Zhang, T.J. Pinnavaia, Angew. Chem. Int. Ed. 40 (2001) 1255.
[23] Z. Zhang, Y. Han, L. Zhu, R. Wang, Y. Yu, S. Qiu, D. Zhao, F. Xiao, Angew. Chem. Int. Ed. 40 (2001) 1258.
[24] Y. Han, F. Xiao, S. Wu, Y. Sun, X. Meng, D. Li, S. Lin, F. Deng, X. Ai, J. Phys. Chem. B 105 (2001) 7963.
[25] Y. Liu, T.J. Pinnavaia, Chem. Mater. 14 (2002) 3.
[26] Y. Han, S. Wu, Y. Sun, D. Li, F. Xiao, Chem. Mater. 14 (2002) 1144.
[27] J. Agundez, I. Diaz, C.M. Alvarez, J.P. Pariente, E. Sastre, Chem. Commun. (2003) 150.
[28] Y. Di, Y. Yu, Y. Sun, X. Yang, S. Lin, M. Zhang, S. Li, F. Xiao, Micropor. Mesopor. Mater. 62 (2003) 221.
[29] L. Sierra, B. Lopez, J. Gil, J.L. Guth, Adv. Mater. 11 (1999) 307.
[30] R. Mokaya, W.Z. Zhou, W. Jones, Chem. Commun. (1999) 51.
[31] Z.T. Zhang, Y. Han, F.S. Xiao, S.L. Qiu, L. Zhu, R.W. Wang, Y. Yu, Z. Zhang, B.S. Zou, Y.Q. Wang, H.P. Sun, D.Y. Zhao, Y. Wei, J. Am. Chem. Soc. 123 (2001) 5014.
[32] S. Sato, G.E. Maciel, J. Mol. Catal. A 101 (1995) 153.
[33] J.M. Thomas, J. Klinowsk, Adv. Catal. 33 (1985) 199.
[34] J.L. Gray, G.E. Maciel, J. Am. Chem. Soc. 103 (1981) 7147.
[35] X.S. Zhao, M.G.Q. Lu, C. Song, J. Mol. Catal. A 191 (2003) 67.
[36] M. Niwa, N. Katada, M. Sawa, Y. Murakami, J. Phys. Chem. 99 (1995) 8812.
[37] A. Gedeon, A. Lassoued, J.L. Bonardet, J. Fraissard, Micropor. Mesopor. Mater. 44–45 (2001) 801.
[38] D.Y. Zhao, C. Nie, Y.M. Zhou, S.J. Xie, L.M. Huang, Q.Z. Li, Catal. Today 68 (2001) 11.
[39] A. Corma, V. Fornes, M.T. Navarro, J. Perez-Pariente, J. Catal. 148 (1994) 569.
[40] J. Aguado, D.P. Serrano, J.M. Escola, Micropor. Mesopor. Mater. 34 (2000) 43.
[41] A. Ghanbari-Siahkali, A. Philippou, A. Garforth, G.S. Cundy, M.W. Anderson, J. Dwyer, J. Mater. Chem. 11 (2001) 569.
[42] Y. Liu, T.J. Pinnavaia, J. Mater. Chem. 14 (2004) 1099.
[43] L. Zhu, F.S. Xiao, Z.T. Zhang, Y.Y. Sun, Y. Han, S.L. Qiu, Catal. Today 68 (2001) 209.